

NJC

Accepted Manuscript



This is an *Accepted Manuscript*, which has been through the Royal Society of Chemistry peer review process and has been accepted for publication.

Accepted Manuscripts are published online shortly after acceptance, before technical editing, formatting and proof reading. Using this free service, authors can make their results available to the community, in citable form, before we publish the edited article. We will replace this *Accepted Manuscript* with the edited and formatted *Advance Article* as soon as it is available.

You can find more information about *Accepted Manuscripts* in the [Information for Authors](#).

Please note that technical editing may introduce minor changes to the text and/or graphics, which may alter content. The journal's standard [Terms & Conditions](#) and the [Ethical guidelines](#) still apply. In no event shall the Royal Society of Chemistry be held responsible for any errors or omissions in this *Accepted Manuscript* or any consequences arising from the use of any information it contains.

ARTICLE TYPE

Carbon Fragments are Ripped off from Graphite oxide Sheets During its Thermal Reduction

Ondřej Jankovský^a, Štěpánka Hrdličková Kučková^b, Martin Pumera^c, Petr Šimek^a, David Sedmidubský^a and Zdeněk Sofer^{**a}

5 Received (in XXX, XXX) Xth XXXXXXXXXX 20XX, Accepted Xth XXXXXXXXXX 20XX

Since the discovery of graphene, many different exfoliation processes of graphite oxide have been reported. Thermal reduction is the most often used method for graphene synthesis. It is a general assumption that during the exfoliation water vapor and carbon mono and dioxide are produced. In this paper it is shown that more complex products are formed during this process. Graphite oxides, prepared according to Hofmann, Hummers, Staudenmaier and Brodie methods, having different C/O ratios, were exposed to thermal shock. Resulting fragments detected by time-of-flight spectrometer exhibit the fragment fingerprints are very similar for all graphite oxides. Our finding challenge general assumption that only basic gasses are formed during thermal exfoliation of graphite oxide. The full understanding of the exfoliation mechanism and products is crucial for reproducible scalable synthesis of reduced graphenes on large scale.

Introduction

Graphene has been intensively studied since the discovery of graphene in 2004 for remarkable electrical, optical and mechanical properties.¹ Thanks to these properties graphene and graphene based materials can be used for energy production and storage,² catalysis,³ photovoltaics⁴ electrochemical sensing⁵ and biosensing,⁶ etc. Graphene can be synthesized by the down to top method which is based on principle of CVD techniques.⁷ The second possibility, top to down method, is based on exfoliation of graphite oxide by the chemical reduction or thermal reduction/exfoliation.⁸

Graphite oxide undergoes thermal reduction and exfoliation during thermal heating shock. Oxygen containing groups of graphite oxide are during this process vaporized and cause extreme increase of interlayer pressure which leads to the exfoliation of individual graphite oxide layers.⁹⁻¹⁰ It was suggested that exfoliation products compose of CO, CO₂ and H₂O. The CO₂/H₂O ratio is dependent on the C/O/H ratio of graphite oxide precursor.¹¹ It is well known that product of exfoliation are highly defective: they contains holes (areas where carbon atoms are missing in honeycomb structure) or heptagon/pentagon defects in structure.¹² Such structure may suggest that also larger fragments of carbon atoms are ripped off from graphene sheet.

Here we wish to challenge the simplistic view that only simple gasses as CO, CO₂ or H₂O are being released as exfoliation products from graphite oxide. We show that much more complex molecules are released from graphite oxide during its exfoliation.

Experimental section

We prepared four different graphite oxides from pure graphite microparticles (2–15 μm, 99.9995%, from Alfa Aesar). Sulfuric acid (98%), nitric acid (68%), fuming nitric acid (>98%), potassium chlorate (99%), potassium permanganate (99.5%), sodium nitrate (99.5%), hydrogen peroxide (30%), hydrochloric acid (37%), silver nitrate (99.5%), barium nitrate (99.5%) and N,N-dimethylformamide (DMF) were obtained from Penta, Czech Republic.

Graphite oxide prepared by the Staudenmaier method¹³ was termed ST-GO. Sulphuric acid (98 %, 87.5 mL) and fuming nitric acid (>98 %, 27 mL) were added to a reaction flask containing a magnetic stir bar. Subsequently, the mixture was cooled to 0 °C and graphite (5 g) was added. The mixture was vigorously stirred to avoid agglomeration and to obtain a homogeneous dispersion. While keeping the reaction flask at 0 °C, potassium chlorate (55 g) was slowly added. Upon the complete dissolution of potassium chlorate, the reaction flask was loosely capped to allow the escape of the gas evolved. Then the mixture was continuously stirred for 96 h at room temperature. The mixture was then poured into deionized water (3 L) and decanted. Graphite oxide was redispersed in HCl solution (5 %, 3 L) to remove sulphate ions and repeatedly centrifuged and redispersed in deionized water until a negative reaction on chloride and sulphate ions was achieved. Graphite oxide slurry was then dried in a vacuum oven.

The second graphite oxide was synthesized similarly to the Hummers method and was termed as HU-GO.¹⁴ Graphite (5 g) and sodium nitrate (2.5 g) were stirred with sulphuric acid (98 %, 115 mL). The mixture was then cooled to 0 °C. Potassium permanganate (15 g) was then added over a period of two hours.

During next four hours, the reaction mixture was allowed to reach room temperature before being heated to 35 °C for 30 min. The reaction mixture was then poured into a flask containing deionized water (250 mL) and heated to 70 °C for 15 minutes. The mixture was then poured into deionized water (1 L). The unreacted potassium permanganate and manganese dioxide were removed by the addition of 3% hydrogen peroxide. The reaction mixture was then allowed to settle and decant. The obtained graphite oxide was then purified by repeated centrifugation and redispersing in deionized water until a negative reaction on sulphate ions was achieved. Graphite oxide slurry was then dried in a vacuum oven.

Graphite oxide prepared according to the Hofmann method was termed HO-GO.¹⁵ Sulfuric acid (98 %, 87.5 mL) and nitric acid (68 %, 27 mL) were added to a reaction flask (Pyrex beaker with thermometer) containing a magnetic stir bar. The mixture was then cooled by immersion in an ice bath for 30 min. Graphite (5 g) was then added to the mixture with vigorous stirring motion. While keeping the reaction flask in the ice bath, potassium chlorate (55 g) was slowly added to the mixture. Upon the complete dissolution of potassium chlorate, the reaction flask was then loosely capped to allow the escape of the gas evolved and the mixture was continuously stirred for 96 hours at room temperature. The mixture was poured into 3 L of deionized water and decanted. Graphite oxide was then redispersed in HCl solution (5 %, 3 L) to remove sulfate ions and repeatedly centrifuged and redispersed in deionized water until a negative reaction on chloride and sulfate ions was achieved. Graphite oxide slurry was then dried in a vacuum oven.

Graphite oxide prepared by the Brodie method¹⁶ was termed BR-GO. Fuming nitric acid (>98 %, 62.5 mL) was added to a reaction flask containing a magnetic stir bar. The mixture was then subsequently cooled to 0 °C and graphite (5 g) was added. The mixture was stirred to obtain a homogeneous dispersion. While keeping the reaction flask at 0 °C, potassium chlorate (25 g) was slowly added to the mixture. Upon the complete dissolution of potassium chlorate, the reaction flask was loosely capped to allow the escape of the gas evolved and the mixture was stirred for 20 h at 40 °C. Upon completion of the reaction, the mixture was poured into 3 L of deionized water and decanted. Graphite oxide was then redispersed in HCl solution (5 %, 3 L) to remove sulphate ions and repeatedly centrifuged and redispersed in deionized water until a negative reaction on chloride ions was achieved. Graphite oxide slurry was then dried in a vacuum oven.

Combustible elemental analysis (CHNS-O) was performed with a PE 2400 Series II CHNS/O Analyzer (Perkin Elmer, USA). In CHN operating mode (the most robust and interference free mode), the instrument employs a classical combustion principle to convert the sample elements to simple gases (CO₂, H₂O and N₂). The PE 2400 analyzer performs automatically combustion and reduction, homogenization of product gases, separation and detection.

SEM microscope *Lyra* (Tescan) with FEG electron source was used for the observation of samples. For SEM measurements the original plate used for laser assisted exfoliation in LDI-TOF was used. Elemental composition and mapping were performed using an energy dispersive spectroscopy (SEM-EDS) analyzer (X-Max^N) with a 20 mm² SDD detector (Oxford instruments) and

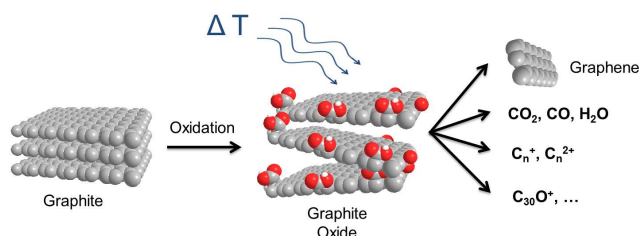
AZtecEnergy software. SEM and SEM-EDS measurements were carried out using a 10 kV electron beam and a working distance 8mm.

inVia Raman microscope (Renishaw, England) in backscattering geometry with CCD detector was used for Raman spectroscopy. DPSS laser (532 nm, 50 mW) with 100x magnification objective was used for the measurement. Instrument calibration was achieved with a silicon reference which gives a peak position at 520 cm⁻¹ and a resolution of less than 1 cm⁻¹. The measurement was performed directly on the holder used for laser assisted exfoliation in LDI-TOF. In order to avoid damage of the measured sample the laser power of 0.5 mW was used.

Samples for laser desorption/ionization with time of flight detector mass spectrometry (LDI-TOF MS) were prepared similarly as described by Kuckova et al.¹⁷ 1 µL of graphite oxide dispersed in DMF (1 mg/mL, 10 min/15 W ultrasonication) were directly dropped on the steel sample plate and air dried. The mass spectra were acquired in positive reflector (for masses in range of 0 - 2000 Da) with mass accuracy 0.4 Da on the mass spectrometer Bruker-Daltonics Biflex IV fitted with a standard nitrogen laser (337 nm, 120 µJ). The spectra were analyzed using the XMASS (Bruker) and mMass software.¹⁸ Each mass spectrum was the result of at least 100 laser pulses. The spectra were calibrated by Pepmix (Bruker Daltonics, Germany). For the graphite oxide exfoliation various laser intensities (20 %, 40 %, 60 %, 80 % and 100 %) were used.

Results and discussion

We prepared four different graphite oxides (GOs) using traditional methods, according to Staudenmaier (ST-GO),¹³ Hofmann (HO-GO),¹⁴ Hummers (HU-GO)¹⁵ and Brodie (BR-GO)¹⁶ and exposed them to rapid heating with consequent analysis of the products by mass spectrometer using time-of-flight detector (TOF). The process is shown in Scheme 1.



Scheme 1 The process of oxidation and subsequent thermal reduction

The morphology of the graphite oxides was investigated by SEM (Fig. 1). GOs exhibited the typical structure formed by the layers of stacked graphite oxide. The micrographs in Figure 2 show the products of thermal exfoliation. Graphene prepared by the laser assisted exfoliation procedure (rapid heating in a vacuum) exhibited a lamellar structure typical for thermally reduced graphite oxide.

During the thermal reduction of the GOs extremely high temperatures with high heating rates are reached locally at the area of the laser beam impact. Such process leads to a decomposition of oxygen containing functional groups which

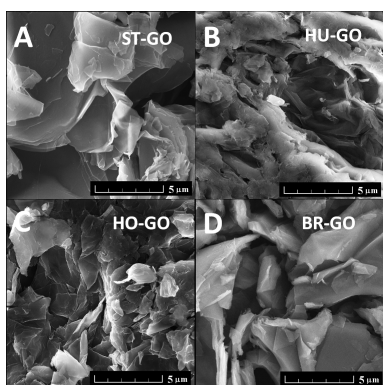


Fig. 1 SEM images of (A) ST-GO, (B) HU-GO, (C) HO-GO and (D) BR-GO.

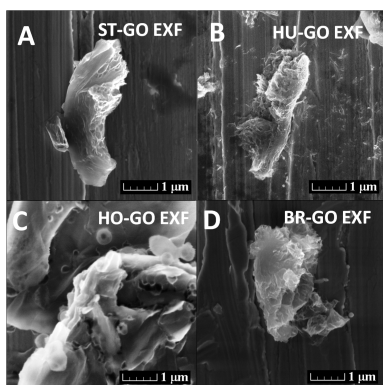


Fig. 2 SEM images after the exfoliation (A) ST-GO EXF, (B) HU-GO EXF, (C) HO-GO EXF and (D) BR-GO EXF.

increases the interlayer pressure causing the exfoliation. During thermal shock temperatures over 1000 °C are locally obtained within the material, however, precise measurements of neither temperature nor heating rate are possible.

The composition (wt.%) of the GOs was determined by the combustible elemental analysis (CHNS-O). ST-GO contained 73.7 wt.% of C, 1.0 wt.% of H and 0.3 wt.% of N and 25.0 wt.% of O; this implies the C/O ratio of ~2.95. Composition of HU-GO was 47.6 wt.% of C, 2.4 wt.% of H, 0.1 wt.% of N and 49.9 wt.% of O, with resulting C/O ratio of ~0.95. HO-GO contained 54.7 wt.% of C, 2.1 wt.% of H, 0.1 wt.% of N and 43.1 wt.% of O with the resulting C/O ratio of ~1.27. BR-GO contained 66.9 wt.% of C, 1.4 wt.% of H, 0.4 wt.% of N and 31.3 wt.% of O with the resulting C/O ratio ~2.14. It is apparent that the different routes of synthesis led to a different degree of oxidation of graphite. Results confirmed a successful synthesis of pure GOs with very low amounts of nitrogen, no sulphur was detected by the elemental analysis.

To confirm results obtained by combustible elemental analysis, we analyzed GOs by SEM-EDS. The composition and obtained C/O ratios are summarized in Table 1. Except for C and O, only trace amount of S (up to 0.3 wt.%) was detected. In comparison with combustible elemental analysis, different result were obtained for the C/O ratios. This fact can be explained by the indirect determination of oxygen in case of combustible elemental analysis. Elemental distribution maps are shown in Figure 3. Very uniform distribution was found in all GOs.

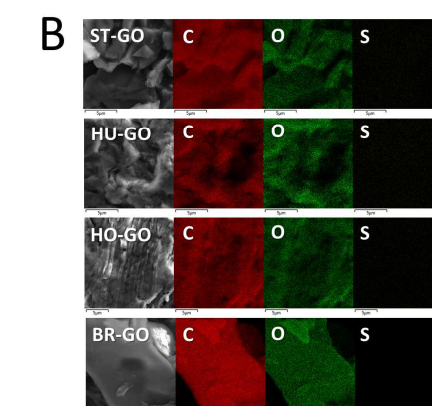
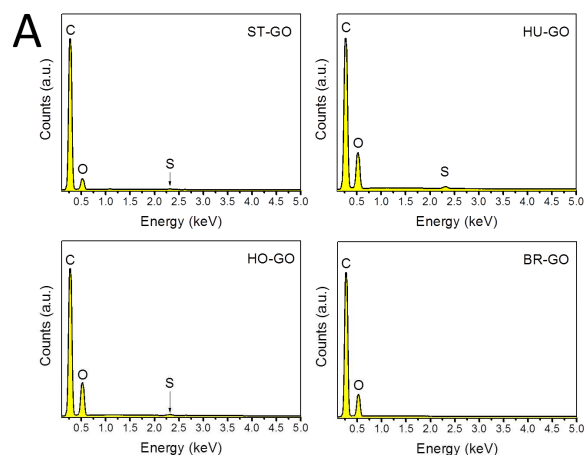


Fig 3 EDS spectra (A) and corresponding elemental maps (B) of graphite oxides.

Table 1 Elemental composition of graphite oxides and corresponding C/O ratios as determined by EDS.

| Sample | C (wt.%) | O (wt.%) | S (wt.%) | C/O ratio |
|--------|----------|----------|----------|-----------|
| ST-GO | 86.8 | 13.1 | 0.1 | 6.63 |
| HU-GO | 74.1 | 25.6 | 0.3 | 2.89 |
| HO-GO | 73.1 | 26.7 | 0.2 | 2.74 |
| BR-GO | 77.8 | 22.2 | 0 | 3.50 |

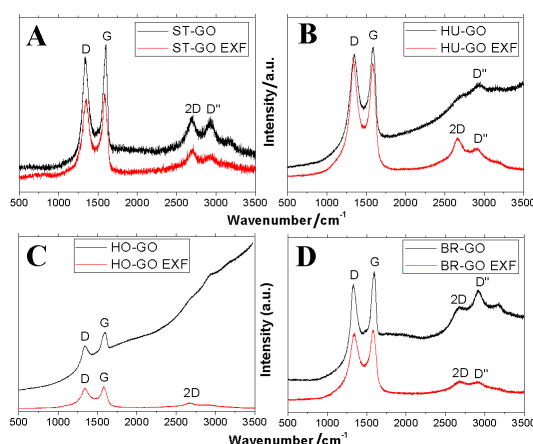


Fig. 4 Raman spectra (A) ST-GO, (B) HU-GO, (C) HO-GO and (D) BR-GO. EXF signs after the thermal reduction (exfoliation).

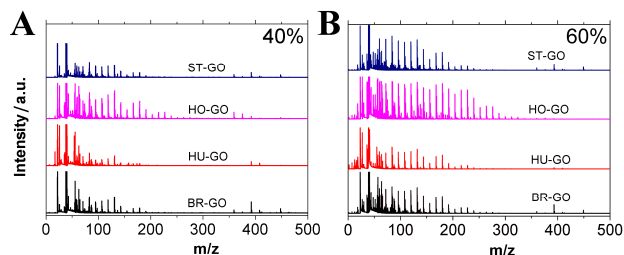


Fig. 5 Mass spectrum of all graphite oxides obtained by (A) 40% of maximum laser energy, (B) 60% of maximum laser energy.

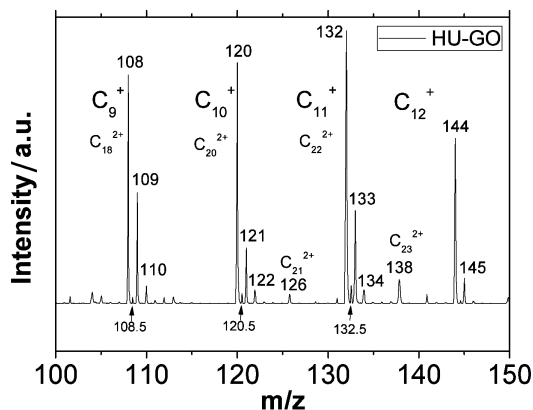


Fig. 6 Detailed mass spectrum in the range of 100 to 150 m/z for HU-GO

We further characterized the materials using Raman spectroscopy. In Figure 4, two major bands were found for all samples. Samples after the thermal reduction are termed EXF (exfoliated). The first band, the D-band associated with sp^3 defects in the sp^2 lattice, gives a signal at $\sim 1350\text{ cm}^{-1}$. The second band, the G-band associated with a pristine sp^2 graphene lattice, gives a signal at $\sim 1560\text{ cm}^{-1}$.¹⁹ Also 2D and D' bands were detected.²⁰ The different intensity of backgrounds is noticeable before and after the exfoliation. Much higher background of sample before the exfoliation is caused by its fluorescence.²¹ From D and G peak intensity ratio it is possible to calculate the crystallite size in the material using equation:²²

$$L_a = 2.4 \times 10^{-10} \times \lambda_{\text{laser}}^4 \times I_G/I_D$$

where I_G/I_D is the ratio of the intensities of the D and G bands respectively and λ_{laser} refers to the laser wavelength (nm).

The D/G ratios and calculated crystallite sizes are summarized in Table 2. Only small changes in the structure of GOs before and after exfoliation were observed. These changes originated from the differences in composition of starting GOs (various concentrations of different oxygen functional groups). HO-GO and BR-GO contain high concentration of epoxide functional groups whose decomposition can form defects within graphene layers which leads to slight decrease of the D/G ratio. On the other hand, exfoliation of ST-GO is accompanied with relatively high increase of D/G ratio. This can originate from decomposition of hydroxyls and other oxygen functional groups presented on graphite oxide surface. HU-GO contains hydroxyl and carboxyl functional groups. Decomposition of carboxyl functional groups does not lead to higher defects concentration on graphene sheets resulting in significant change of the D/G ratio.

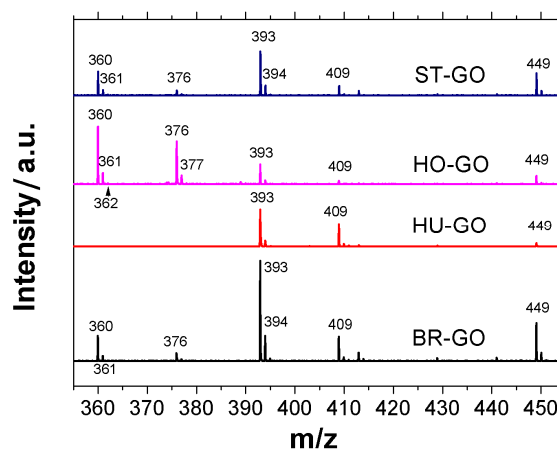


Fig. 7 Detailed mass spectrum in the range of 355 to 455 m/z for all graphite oxides.

Table 2 D/G ratios obtained from Raman spectroscopy and corresponding crystallite sizes of graphite oxides and reduced graphenes (EXF).

| Sample | D/G ratio | L_a (nm) |
|-----------|-----------|------------|
| ST-GO | 0.72 | 26.70 |
| ST-GO EXF | 0.93 | 20.67 |
| HO-GO | 1.01 | 19.03 |
| HO-GO EX | 0.94 | 20.45 |
| HU-GO | 0.97 | 19.82 |
| HU-GO EXF | 1.06 | 18.13 |
| BR-GO | 0.99 | 19.40 |
| BR-GO EXF | 0.96 | 20.01 |

To investigate the products of thermal reduction, time of flight mass spectrometry was performed for 20, 40, 60, 80 and 100 % of laser power output (120 μJ). At high energies (80 and 100 %) only small carbon clusters with m/z lower than 100 were generated. Spectra obtained from 40 % and 60 % of laser output were the most suitable for further analysis to investigate thermal reduction process (Fig. 5). All GOs generated almost similar mass spectra, they differed mostly in amounts of generated ions. At 40 % of laser energy higher yield of heavier ions was observed, while at 60 % of laser output more ions with m/z lower than 300 were formed. H_2O , CO_2 , Na^+ , K^+ and various organic compounds with different C/O/H ratios were detected at m/z lower than 70 in all samples. At higher m/z the presence of carbon clusters C_6^+ , C_7^+ , C_8^+ , etc. was evident in all GOs.

A detail of HU-GO spectrum with C_9^+ , C_{10}^+ , C_{11}^+ and C_{12}^+ is presented in Figure 6. Also the presence of carbon clusters C_{18}^{2+} , C_{20}^{2+} , C_{21}^{2+} , C_{22}^{2+} and C_{23}^{2+} was proved from m/z values 108.5, 120.5, 126, 132.5 and 138, respectively. Similar results were obtained previously,²¹ where series of carbon clusters were also obtained from graphitic matrix.

ARTICLE TYPE

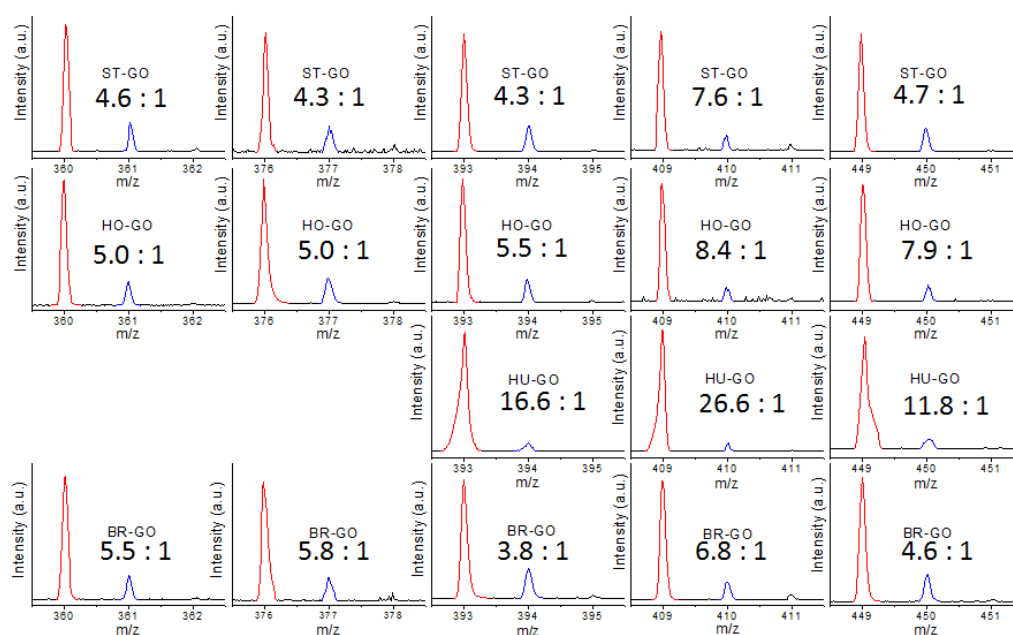


Fig. 8 The detail of mass spectra for the clusters with m/z 360, 376, 393, 409 and 449 for various graphite oxides. The ratios of peak areas were calculated for each cluster.

Spectra of all four GOs with m/z from 355 to 455 are shown in Figure 7 and high resolution details of individual detected peaks are illustrated in Figure 8. While standard FWHM analysis is not suitable for $^{12}\text{C}/^{13}\text{C}$ isotopic ratio investigation, the ratios of $(m/z) : (m/z)+1$ were calculated from peak areas (Figure 8). Let us note that LDI-TOF spectroscopy is not accurate compared to other mass spectroscopy techniques.

Detected peak at $360\ m/z$ in ST-GO, HO-GO and BR-GO most corresponded to $^{12}\text{C}_{30}^+$ ion. The peak at $m/z = 361$ was formed due to the presence of ^{13}C in the form $^{12}\text{C}_{29}^{13}\text{C}_1^+$. Also a weak peak at $m/z = 362$ was found corresponding to the $^{12}\text{C}_{28}^{13}\text{C}_2^+$. The ratio of m/z 360 and 361 indicates the presence of pure C_{30}^+ ion. Such carbon cluster was already reported in the literature.²³ Also Bowers et al. reported formation of stable planar bi-, tri- and tetra-cyclic rings for C_{20} , C_{30} and C_{40} .²⁴

At $376\ m/z$ there is another peak present in ST-GO, HO-GO and BR-GO, which is connected to the former one at 360. It can be explained by the presence of ion C_{30}O^+ . The formation of C_{30}^+ and C_{30}O^+ was not observed for HU-GO. The formation of heteroatom molecular clusters is strongly related to the chemical composition of graphite oxide. Presence of such peak can be also used as a fingerprint to distinguish between graphite oxide prepared by methods using chlorate and permanganate oxidation agents.

Also two major peaks at 393 and $409\ m/z$ were detected differing by one oxygen atom. The molecular cluster with $393\ m/z$ had most probably the composition of $\text{C}_{30}\text{O}_2\text{H}_1^+$. The larger cluster with $409\ m/z$ had a composition with one more oxygen atom and corresponded to the $\text{C}_{30}\text{O}_3\text{H}_1^+$.

The last peak at $449\ m/z$ corresponded to a composition of $\text{C}_{36}\text{O}_1\text{H}_1^+$ with the highest intensity for BR-GO and ST-GO. This is related to the differences in graphite oxide composition where BR-GO and ST-GO contain only negligible concentration of carboxylic acid functionalities and dominantly contain hydroxyl and epoxide groups. The oxygen and hydrogen containing clusters can be formed in the gas phase by charge transfer reactions with dominant product of graphite oxide exfoliation (CO_2 , CO and H_2O). The formation of such clusters in the presence of carbon dioxide and water vapor was reported in the case of graphite interaction with laser beam.²⁵

The detailed analysis of peak areas of m/z and $m/z+1$ peaks showed different behavior for HU-GO compared to other GOs (Fig. 8). The ratio of m/z to $m/z+1$ was in the range of about 4:1 up to 8:1 for ST-GO, HO-GO and BR-GO, while in the case of HU-GO the ratio was much higher. This can indicate the deviation of the cluster composition. Due to the different composition of HU-GO (HU-GO was prepared by permanganate based oxidation method) the reduction of $394\ m/z$, $410\ m/z$ and $450\ m/z$ intensities can be assigned to the higher concentration of oxygen with in the cluster where each four ^{12}C atoms can be substituted with three ^{16}O atoms; however the precise explanation of such results is challenging.

In the region $450 - 2000\ m/z$ no ions were detected. This is a significantly different behavior compared to mass spectra obtained by laser ablation of graphite. We can conclude that the presence of oxygen functionalities in graphite oxide prevents the formation of higher carbon clusters or fullerenes.

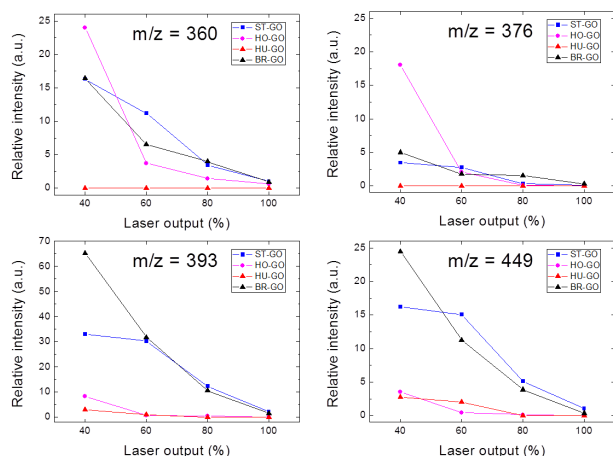


Fig. 9 Relative abundance of individual carbon clusters for various laser energies.

We also studied the relationship between the intensity of laser and the amount of large carbon clusters formed. Relatively low values of the maximal laser energy (~40%) were the most suitable to reach the highest yield of large clusters. While 20% energy (24 μ J) was not sufficient for the exfoliation, energies 80 and 100% led dominantly to the formation of small carbon clusters. Comparison of the obtained results is shown in Figure 9. The relative yield of four clusters with the highest abundance ($m/z = 360, 376, 409$ and 449) was related to the total amount of carbon cluster C^{7+} which was present in all GOs for 40, 60, 80 and 100% of laser power outputs.

Conclusions

We demonstrated that during rapid heating of graphite oxide, large amount of complex ions was generated. The mass spectra of exfoliation products of all investigated graphite oxides prepared by various methods show almost identical fingerprint with carbon cluster containing up to 36 carbon atoms. Only small differences in mass spectra of exfoliation products were observed between the graphite oxide prepared by chlorate based methods and permanganate methods. In the case of graphite oxide prepared by Hummers method molecular clusters $C_{30}O^+$ and C_{30}^+ were not detected. LDI-TOF MS can be used for the fast identification of method used for graphite oxide synthesis. Characteristic mass spectra of all graphite oxides allowed applications of such materials like matrix for characterization of various bio-macromolecules.

Acknowledgement

O.J., P.Š. and Z.S. were supported by Specific University Research grant (MSMT No 20/2014). M.P. thanks NAP (NTU) grant for funding.

Notes and references

- ^a Institute of Chemical Technology, Department of Inorganic Chemistry, 166 28 Prague 6, Czech Republic, E-mail:zdenek.sofer@vscht.cz; Fax: +420 22431-0422
- ^b Institute of Chemical Technology, Department of Biochemistry and Microbiology, 166 28 Prague 6, Czech Republic, E-mail: Stepanka.Hrdlickova.Kuckova@vscht.cz
- ^c Division of Chemistry & Biological Chemistry, School of Physical and Mathematical Sciences, Nanyang Technological University, Singapore, 637371, Singapore. E-mail: pumera@ntu.edu.sg; Fax: +65 6791-1961
- 1 A. K. Geim, K. S. Novoselov, *Nat. Mater.*, 2007, **6**, 183-191.
- 2 M. Pumera, *Energy Environ. Sci.*, 2011, **4**, 668-674.
- 3 C. Huang, H. Bai, C. Li, G. Shi, *Chem. Commun.*, 2011, **47**, 4962-4964.
- 4 X. Wang, L. Zhi, K. Mullen, *Nano Lett.*, 2007, **8**, 323-327.
- 5 H. S. Poh, A. Ambrosi, C. K. Chua, M. Pumera, *J. Phys. Chem. C* 2011, **115**, 17647-17650.
- 6 A. Bonanni, M. Pumera, *ACS Nano*, 2011, **5**, 2356-2361.
- 7 S. Bae, H. Kim, Y. Lee, X. Xu, J.-S. Park, Y. Zheng, J. Balakrishnan, T. Lei, H. R. Kim, Y. I. Song, Y.-J. Kim, K. S. Kim, B. Özyilmaz, J.-H. Ahn, B. H. Hong, S. Iijima, *Nat. Nanotech.*, 2010, **5**, 574-578.
- 8 M. Acik, Y. J. Chabal, *J. Mater. Sci. Res.*, 2013, **2**, 101-112.
- 9 M. J. McAllister, *Chem. Mater.*, 2007, **19**, 4396-4404.
- 10 W. Chen, L. Yan, P. R. Bangal, *Carbon*, 2010, **48**, 1146-1152.
- 11 H. L. Poh, F. Sanek, A. Ambrosi, G. Zhao, Z. Sofer, M. Pumera, *Nanoscale*, 2012, **4**, 3515-3522.
- 12 C. Gómez-Navarro, J. C. Meyer, R. S. Sundaram, A. Chuvilin, S. Kurasch, M. Burghard, K. Kern, U. Kaiser, *Nano Lett.*, 2010, **10**, 1144-1148.
- 13 L. Staudenmaier, *Ber. Dtsch. Chem. Ges.*, 1898, **31**, 1481-1487.
- 14 W. S. Hummers, R. E. Offeman, *J. Am. Chem. Soc.*, 1958, **80**, 1339.
- 15 W. S. Hummers and R. E. Offeman, *J. Am. Chem. Soc.*, 1958, **80**, 1339-1339.
- 16 B. C. Brodie, *Ann. Chim. Phys.*, 1860, **59**, 466-472.
- 17 S. Kuckova, R. Hynek, I. Nemeč, M. Kodicek, J. Jehlicka, *Surf. Interface Anal.*, 2012, **44**, 963-967.
- 18 M. Strohalm, M. Hassman, B. Kosata, M. Kodicek, *Rapid Commun. Mass Spectrom.*, 2008, **22**, 905-908.
- 19 D. R. Dreyer, R. S. Ruoff, C. W. Bielawski, *Angew. Chem., Int. Ed.*, 2010, **49**, 9336-9344.
- 20 M. S. Dresselhaus, A. Jorio, M. Hofmann, G. Dresselhaus, R. Saito, *Nano Lett.*, 2010, **10**, 751-758.
- 21 K. P. Loh, Q. Bao, G. Eda, M. Chhowalla, *Nat. Chem.*, 2010, **2**, 1015-1024.
- 22 L. G. Cançado, K. Takai, T. Enoki, M. Endo, Y. A. Kim, H. Mizusaki, A. Jorio, L. N. Coelho, R. Magalhães-Paniago, M. A. Pimenta, *Appl. Phys. Lett.*, 2006, **88**, 163106.
- 23 A. Crecelius, M. R. Clench, D. S. Richards, V. Parr, *J. Chromatogr. A*, 2002, **958**, 249-260.
- 24 M. T. Bowers, P. R. Kemper, G. von Helden, P. A. M. van Koppen, *Science*, 1993, **260**, 1446-1451.
- 25 R. Ramanathan, J. A. Zimmerman, J. R. Eyler, *J. Chem. Phys.*, 1993, **98**, 7838-7845.